

Stability of Square Plate with Concentric Cutout

B. S. Jayashankarbabu, Karisiddappa

Abstract—The finite element method is used to obtain the elastic buckling load factor for square isotropic plate containing circular, square and rectangular cutouts. ANSYS commercial finite element software had been used in the study. The applied inplane loads considered are uniaxial and biaxial compressions. In all the cases the load is distributed uniformly along the plate outer edges. The effects of the size and shape of concentric cutouts with different plate thickness ratios and the influence of plate edge conditions, such as SSSS, CCCC and mixed boundary condition SCSC on the plate buckling strength have been considered in the analysis.

Keywords—Concentric cutout, Elastic buckling, Finite element method, Inplane loads, Thickness ratio.

I. INTRODUCTION

STEEL plates are often used as the main components of steel structures such as webs of plate girders, box girders, ship decks and hulls, and platforms on oil rigs. Perforations are often included in the stressed skin cover of air plane wings. In plates cutouts are provided to decrease the self-weight, to provide access, services and even aesthetics. When these structures are loaded, the presence of cutouts will cause changes in the member mechanical properties, consequently there will be change in the buckling characteristics of the plate as well as on the ultimate load capacity of the structure. The shape of a cutout, different plate boundary conditions, thickness ratios of the plate and the type of load applied, influence the performance of plates. However, though the cutouts are provided to achieve certain structural advantages, it is worth to mention here that they may inadvertently affect the stability of the plate component in the form of buckling. This always can be accomplished by thicker plate but the design solution will not be economical in terms of the weight of material used. It is possible to design an adequately strong and rigid structural plate element by keeping its thickness as small as possible. Hence the study of plate stability behavior is of paramount importance. Although much information is available regarding the buckling strength of perforated plate under simply supported boundary conditions, very less information is available in the literature concerning the influence of different shape and size of cutout at centre and plate thickness on the elastic buckling strength of plate, this is because of the difficulties involved in determining the buckling strength of such plate by using classical methods of analysis. Owing to the complexity of the problem caused by lack of symmetry in the plate thicknesses and the cutout, it

appears that a numerical method such as the finite element method would be the most suitable for solving this problem. The stability of plate under various compressive loading and boundary conditions has been the subject and studied by Herrmann and Armenakas [6], Timoshenko and Gere [13] and many others. Thin plate theory is based on several approximations, the most important of which is the neglect of transverse shear deformations. The errors of such a theory naturally increase as the thickness of plate increases, Srinivas and Rao [11]. Chiang-Nan Chang and Feung-Kung Chiang [3] observed the change of mechanical behaviors due to the interior holes cut from plate structures and proved the importance to study the buckling behaviors to avoid the structure instability. They used FEM and considering the incremental deformation concept to study the buckling behavior of Mindlin thick plate with interior cutout for different boundaries and different opening ratios. Christopher J. Brown, Alan L. Yettram and Mark Burnett [4] have used the conjugate load/displacement method to predict the elastic buckling load of square plate with centrally located rectangular holes under different types of loads. Shakerley T. M. and Brown C. J. [9] have used the conjugate load/displacement method to study the effect of eccentricity of a square or rectangular hole on the elastic buckling of a square plate subjected to axial or shear loads. Shanmugam, Thevendran and Tan [10] have used FEM to develop a design formula to determine the ultimate load carrying capacity of axially compressed square plate with centrally located perforations, circular or square. They concluded that the ultimate load capacity of the square perforated plate is affected significantly by the hole size and the plate slenderness ratio. Aydin Komur and Mustafas Sonmez [2] have used the FEM to study the effect of cutout location on elastic buckling of rectangular plates under linearly varying inplane normal loads with a circular cutout. El-Sawy and Nazmy [5] have used the FEM to investigate the effect of plate aspect ratio and hole location on elastic buckling of uniaxially loaded rectangular plates with eccentric holes with simply supported edges in the out-of-plane direction. The study concluded that the use of a rectangular hole with curved corners, with its short dimension positioned along the longitudinal direction of the plate is better option than using a circular hole from the plate stability point of view. Ultimate strength of square plate with rectangular opening under axial compression using non-linear finite element analysis was studied by Suneel Kumar, Alagusundaramoorthy and Sundaravadevelu [12]. A general purpose finite element software ANSYS was used for carrying out the study. Jeom Kee Paik [7] studied the ultimate strength of perforated steel plate under combined biaxial compression and edge shear loads for the circular cutout located at the centre of the plate. A series of ANSYS elastic-plastic large

Jayashankarbabu B. S. is Associate Professor, Dept. of Civil Eng., P.E.S. College of Engineering, Mandya-571401, Karnataka, India (e-mail: jsbabupesce@gmail.com).

Dr. Karisiddappa is Principal, Govt. Engineering College, Hassan, Karnataka, India (e-mail: karisiddappamce@yahoo.com).

deflection finite element analysis has been carried out on perforated steel plate with varying plate thicknesses.

In the present paper it has been attempted to investigate the effect of the size of concentric circular, square and rectangular cutouts and the impact of thickness of the plate on the buckling load of all-round simply supported (SSSS), clamped (CCCC) and SCSC plate boundary condition on the isotropic square plate subjected to uniform inplane uniaxial and biaxial compression loadings. To carry out the study, ANSYS software has been used with 8SHELL93 element [1]. The finite element mesh used to model the plate has been decided upon carrying out a series of convergence tests and considered 10 x 10 mesh shows nearly the accurate results hence it has been used in the analysis.

II. PROBLEM DEFINITION

The problem of elastic buckling of a square plate subjected to uniaxial and biaxial compression loadings along its ends in Fig. 1 having different cutout such as circular, square and rectangular shapes, different boundary conditions such as simply supported, clamped and SCSC. The plate has thickness h and dimensions A and B in x and y -directions, respectively and circular cutout with diameter d , square and rectangular cutouts of size $a \times b$. Here concentric cutout ratio is defined as the ratio of size of cutout to side of plate. The buckling load factor k is assessed with respect to the concentric cutout; vary between 0.1 and 0.6 and also with respect to the plate thickness ratio η , 0.01 to 0.3. It is known that a square plate with all clamped fixed boundary conditions is more stable than the same plate with all simply supported boundary conditions. Since the actual boundary conditions for a real plate may be somewhere between the all clamped and the all simply supported extremities and hence in addition to the above two, the following mixed plate boundary conditions such as SCSC has been considered.

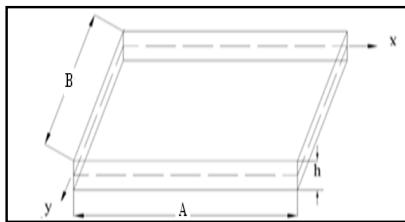


Fig. 1 Geometry of the plate

III. FINITE ELEMENT ANALYSIS PROCEDURE

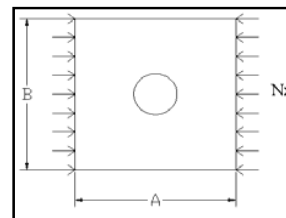
The commercial multipurpose finite element software program ANSYS was employed in this study. 8SHELL93 element is used to model the perforated plate because it shows satisfactory performance in verification work previously described by El-Sawy [5]. The elastic SHELL93 element has eight nodes possessing six degrees of freedom per node. The material of the plate was assumed to be homogeneous, isotropic and elastic. The material properties for Young's modulus $E=210924\text{N/mm}^2$ and Poisson's ratio $\mu=0.3$ were used.

A. Buckling of Simply Supported Thick Plate under Uniaxial Compression

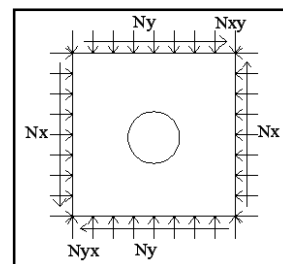
R. D. Mindlin in 1951 published the famous thick plate theory. This two dimensional theory of flexural motions of isotropic elastic plates is deduced from the three dimensional equations of elasticity. The theory includes the effects of rotary inertia and shear in the same manner as Timoshenko's one dimensional theory of bars [13]. The following assumptions are also applied.

- 1) The straight line that is vertical to the neutral surface before deformation remains straight but not necessarily vertical to the neutral surface after deformation.
- 2) Displacement is small so that small deformation theory can be applied.
- 3) Normal stress in the z -direction is neglected.
- 4) Body force is neglected.

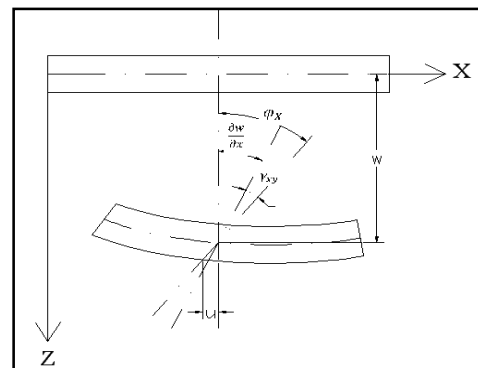
A plate of size A and B subjected to a system of general external inplane loadings, shown in Fig. 2 has been considered.



(a) Geometry



(b) Inplane stress resultants



(c) Thick plate deformation

Fig. 2 Plate with opening and inplane stress resultants

The internal stress resultants at the edges of an element due to the external inplane loads be N_x , N_y and N_{xy} as depicted in Fig. 2. The total potential energy of the plate due to flexure and the work done by the membrane stress resultants, taking the shear deformation into account may be written as:

$$U = \frac{1}{2} A_p \int_0^1 \left\{ \left[\frac{\partial^2 w}{\partial x^2} + \frac{\partial^2 w}{\partial y^2} \right]^2 - 2(1-\mu) \left[\frac{\partial^2 w}{\partial x^2} + \frac{\partial^2 w}{\partial y^2} - \left(\frac{\partial^2 w}{\partial x \partial y} \right)^2 \right] \right\} dA \\ + \frac{D}{2} A_p \int_0^1 \frac{6\chi(1-\mu)}{h^2} [\phi_x^2 + \phi_y^2] dA + \frac{1}{2} A_p \int_0^1 \left[N_x \left\{ \left(\frac{\partial u}{\partial x} \right)^2 + \left(\frac{\partial v}{\partial x} \right)^2 + \left(\frac{\partial w}{\partial x} \right)^2 \right\} \right. \\ \left. + N_y \left\{ \left(\frac{\partial u}{\partial y} \right)^2 + \left(\frac{\partial v}{\partial y} \right)^2 + \left(\frac{\partial w}{\partial y} \right)^2 \right\} + 2N_{xy} \left\{ \frac{\partial u}{\partial y} \frac{\partial u}{\partial z} + \frac{\partial v}{\partial z} \frac{\partial v}{\partial x} + \frac{\partial w}{\partial x} \frac{\partial w}{\partial y} \right\} \right] dA \quad (1)$$

where χ is the Reissner's shear correction factor, A_p is the area of the plate including the cutout, A_c is the area of the cutout, Φ_x , Φ_y are average shear strains, N_x , N_y , N_{xy} are inplane stress resultants and D is the flexural rigidity of the plate. The stiffness matrix $[K]$ is the combination of $[K_b]$ and $[K_s]$ such that $[K] = [K_b] + [K_s]$, in which the former is due to flexure [4] and the later is due to the work associated with the inplane stress resultants. Thus static buckling equilibrium equation becomes,

$$[[K_b] - [K_s]] \{q\} = 0 \quad (2)$$

The stress resultants N_x , N_y and N_{xy} are functions of geometrical ordinates (X,Y) for the plate and depend upon the magnitude of the external inplane loads, $\{q\}$ is nodal displacement vector. Choosing a factor λ , by which the inplane stress resultants can be gradually increased, (2) may be written as.

$$[[K_b] - \lambda [K_s]] \{q\} = 0, \text{ in which } [K_s] = \lambda [K_\sigma] \quad (3)$$

The Eigen values of (3) give the critical loads λ_{ij} of the plate under investigation. The lowest Eigen value corresponds to the fundamental critical load λ_{cr} .

Let P_{cr} be the critical buckling load and by replacing λ by P_{cr} , the governing equation for the static stability problem modified to

$$[[K_b] - P_{cr} [K_\sigma]] \{q\} = 0 \quad (4)$$

The general equation of stability given in (4) contains the structural properties in matrix form, viz., $[K_b]$ and $[K_s]$. The very basic assumption in the derivation of these equations is that the displacement model of the entire structure which satisfies the equilibrium equations and compatibility conditions. Developing such a true displacement model is a tedious exercise. In the present study an alternate method, using the finite element technique through ANSYS software has been used.

IV. DISCUSSION OF THE RESULTS

Results on the effect of shape and size of circular, square and rectangular cutouts and plate thickness ratio on the

buckling load factor k of the square plate having SSSS, CCCC and SCSC plate boundary conditions, subjected to inplane uniaxial and biaxial compression loading cases are presented and discussed in this section. Here, the concentric cutout ratio, defined as the ratio of side of the cutout to plate side, for circular (β) and square (δ) lies between 0.1 – 0.6 and for rectangular cutout it is 0.1–0.5, along x direction (γ) and along y direction (γ'). The thickness ratio (η) defined as the ratio of plate thickness to the plate side and varies from 0.01 - 0.3.

The critical buckling load factor is non-dimensionalised and represented as follows:

$$k = \frac{(N_{cr})B^2}{\pi^2 D} \quad (5)$$

where, k = the buckling load factor.

N_{cr} = the critical buckling load.

D = Plate flexural rigidity = $\frac{Eh^3}{12(1-\mu^2)}$

μ = Poisson's ratio of isotropic plate.

h = thickness of the plate.

A. Comparative Study

In order to verify the present analysis, a comparison with existing results in the literature on buckling of square plate with and without cutout has been performed. The results of present study with the available values are tabulated in Tables I-III. It can be observed that the results from the present work are in good agreement with the established work.

TABLE I
COMPARISON OF BUCKLING LOAD FACTOR (K) FOR ISOTROPIC SOLID PLATE
SUBJECTED TO INPLANE UNIAXIAL COMPRESSION LOAD

Sl. No	Boundary condition	Thickness ratio (η)	Buckling load factor(k)	Reference value
1	SSSS	0.01	3.99	4.00[13]
		0.05	3.94	3.91[11]
		0.10	3.78	3.74[11]
		0.15	3.55	Present study
		0.20	3.26	3.15[11]
		0.25	2.96	Present study
		0.30	2.18	Present study
		0.01	10.4	10.07[13]
2	CCCC	0.05	9.81	Present study
		0.10	8.49	Present study
		0.15	6.96	Present study
		0.20	5.55	Present study
		0.25	4.36	Present study
		0.30	3.43	Present study

TABLE II

COMPARISON OF BUCKLING LOAD FACTOR (K) FOR ISOTROPIC THIN PLATE WITH CONCENTRIC CIRCULAR CUTOUT SUBJECTED TO INPLANE UNIAXIAL COMPRESSION LOAD

Sl. no	Boundary condition	Cutout ratio β	Buckling load factor(k)	Reference value
1	SSSS	0.1	3.8434	3.80[8]
2		0.2	3.5310	3.50[8]
3		0.3	3.2642	3.20[8]
4		0.4	3.1124	3.10[8]
5		0.5	3.0460	2.99[8]
6		0.6	2.8547	Present study

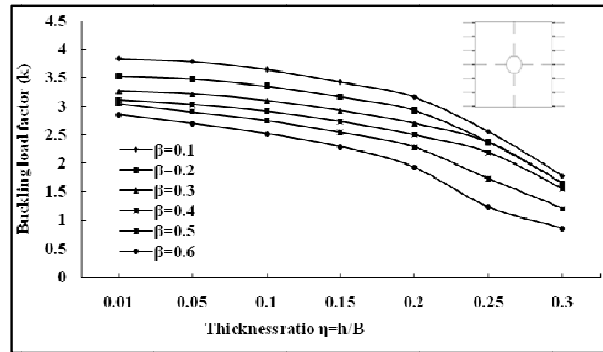
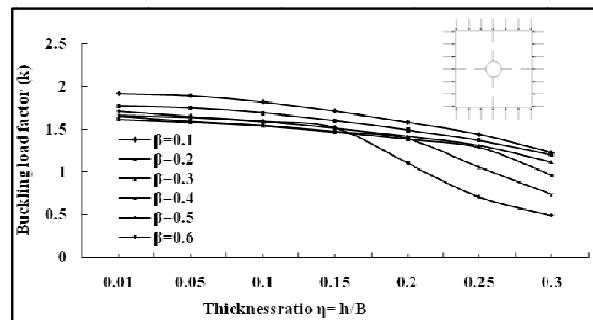
TABLE III

COMPARISON OF BUCKLING LOAD FACTOR (K) FOR ISOTROPIC THIN PLATE WITH CONCENTRIC SQUARE CUTOUT SUBJECTED TO INPLANE BIAXIAL COMPRESSION LOAD

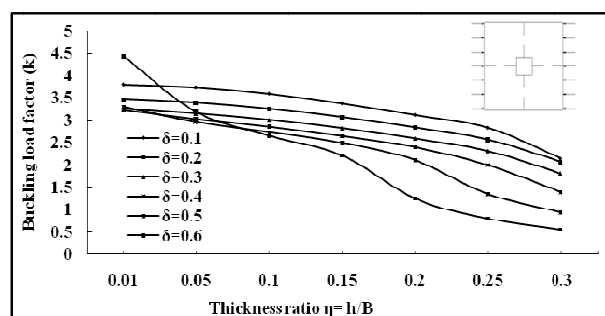
Sl. No	Boundary condition	Ratio of size of hole to plate side $\delta=b/A$	Buckling load factor(k)	Reference value
1	SSSS	0	1.9980	2.0[13]
		0.1	1.9051	Present study
		0.2	1.7496	Present study
		0.25	1.6986	1.65[14]
		0.3	1.6684	Present study
		0.4	1.7028	Present study
		0.5	1.8891	1.55[14]
2	CCCC	0.6	2.5182	Present study
		0	5.287	5.32[14]
		0.1	5.2068	Present study
		0.2	5.0834	Present study
		0.25	6.5036	5.28[14]
		0.3	5.0016	Present study
		0.4	4.9551	Present study
3	SCSC	0.5	5.4765	8.61[14]
		0.6	5.5579	Present study
		0	3.0867	3.84[14]
		0.1	2.9833	Present study
		0.2	2.8410	Present study
		0.25	2.8144	3.52[14]
		0.3	2.8075	Present study
		0.4	2.8548	Present study
		0.5	3.1868	4.12[14]
		0.6	3.5628	Present study

B. Case of Plate with Simply Supported Boundary Conditions

Figs. 3-10 show the variation of the buckling load factor k for the plate with different cutout ratios having SSSS boundary conditions subjected to inplane uniaxial and biaxial compression loading cases. In all these figures the variations of the buckling load factor k are plotted against thickness ratios η and cutout ratios. It can be noticed in these figures that, buckling behavior of the plate is greatly affected by increase in thickness ratios.

Fig. 3 Variation of k with η and β for uniaxial compressionFig. 4 Variation of k with η and β for biaxial compression

In Fig. 3, buckling load factor k decreases gradually up to thickness ratio $\eta < 0.2$ for all circular cutout ratios β . When $\eta > 0.2$, k reduction is in higher magnitude i.e., in the range of 25% to 52%. Fig. 4 represents the variation of buckling load factor k for square plate having concentric circular cutout subjected to biaxial loading. In case of biaxial loading, k value is found to be almost half of that of uniaxial compression value. This may be due to stiffening of the plate in both x and y directions. It is noticed that k always decreases with increase in η and β and this decrease is steeper for $\beta > 0.3$ and $\eta > 0.15$. When $\beta = 0.6$ and $\eta = 0.3$, 60% of reduction in k is observed to that of $\beta = 0.1$.

Fig. 5 Variation of k with η and δ for uniaxial compression

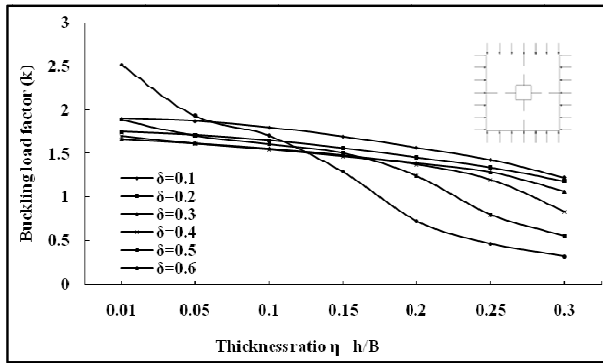
Fig. 6 Variation of k with η and δ for biaxial compression

Fig. 5 represents the variation of buckling load factor k for square plate with concentric square cutout ratios δ , subjected to uniaxial loading. Here, the value of k is 10% less than that of circular cutout and k value decreases as δ and η increases, except at $\delta=0.6$ and for $\eta=0.01$, an increase of 16.33% in k value can be observed compared to $\delta=0.1$. This does not necessarily mean that the increase in buckling strength of the plate at $\delta=0.6$, plate already loosened its strength to react to that stage; because plate strength corresponds to removal of plate material. When the cutout ratio becomes large and $\eta > 0.15$, the reduction is more rapid and it is less than 50% for $\delta \leq 0.3$ for all values of η and it is more than 50% for $\delta > 0.3$. Fig. 6 represents the variation of buckling load factor k for square plate having concentric square cutout, subjected to biaxial loading. Here, k value is 50% compared to uniaxial loading case. It is noticed that the variation of k is very less for δ up to 0.3 with respect to η values, but high variation is noticed when $\delta > 0.3$. k decrease is unpredictable at $\delta=0.6$ and k reduction is noticed in the magnitude of 54%, 67% and 74% when $\eta=0.2$, 0.25 and 0.3 respectively.

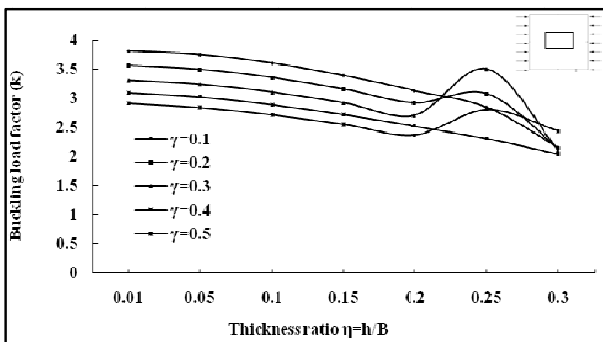
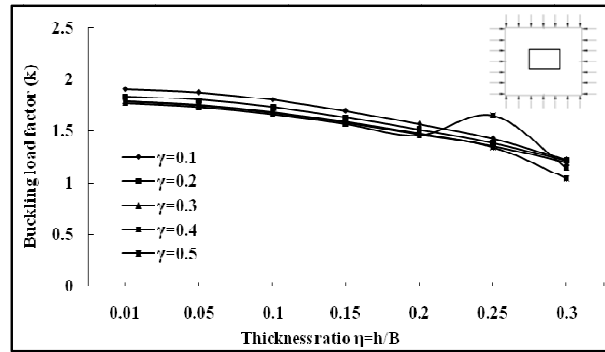
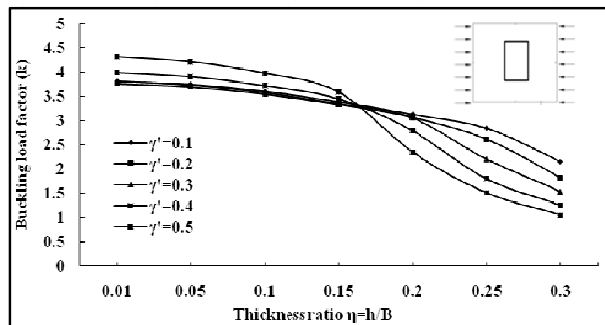
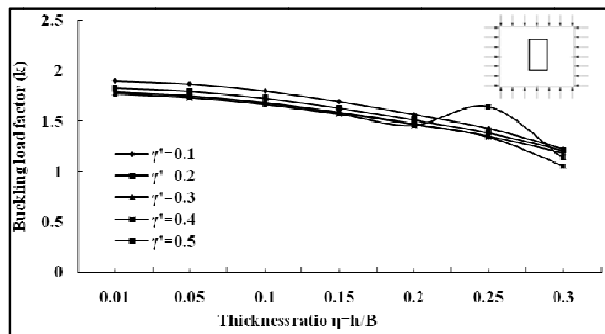
Fig. 7 Variation of k with η and γ for uniaxial compressionFig. 8 Variation of k with η and γ for biaxial compression

Fig. 7 represents the variation of buckling load factor k for square plate having concentric rectangular cutout along x -direction γ subjected to uniaxial loading. Here, the decrease in k value is gradual when compared to circular and square cutout. k always decreases as η and γ increases except for η lies between 0.15 to 0.25 and $\gamma=0.2$, 0.3 and 0.5 where a sudden variation in k value can be observed.

Fig. 9 Variation of k with η and γ' for uniaxial compressionFig. 10 Variation of k with η and γ' for biaxial compression

Figs. 8 and 10 represent the variation of buckling load factor k for square plate having concentric rectangular cutout along x and y -directions, γ and γ' , respectively under biaxial loading. Here, the value of k is half of that of uniaxial loading case and the variation of k is very less as η and γ' increases. This shows that thickness ratio and cutout ratios have less significant effect on the k . In case of biaxial loading, rectangular cutout along x and y -directions, k remains almost

same. Fig. 9 represents the variation of buckling load factor k for square plate having concentric rectangular cutout along y -direction subjected to uniaxial loading. It is noticed that as η increases k decreases and this decrease is significant when $\gamma' > 0.3$, and it is noticed that reduction of k is up to the range 43.5%, 51%, 60%, 69% and 76% with the increase of γ' from 0.1 to 0.5 with respect to $\eta=0.01$ to 0.3. It is noticed from the above figures that, for small cutout ratios, there is a little effect of thickness ratio η up to 0.15. But when cutout ratio becomes larger, increasing the plate thickness ratio shows significant effect on the buckling strength of the plate.

C. Case of Plate with Clamped Boundary Conditions

Figs. 11-18 show the variation of the buckling load factor k for the plate with different cutout ratios having CCCC boundary conditions subjected to inplane uniaxial and biaxial compression loading cases. In all these figures the variation of the buckling load factor k are plotted against thickness ratio η and cutout ratios. It can be noticed in these figures that, buckling behavior of the plate is greatly affected by increase in plate thickness ratios.

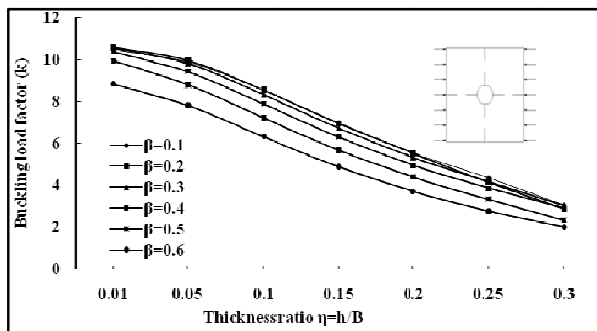


Fig. 11 Variation of k with η and β for uniaxial compression

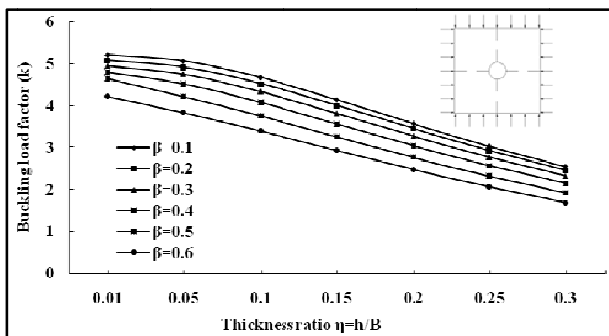


Fig. 12 Variation of k with η and β for biaxial compression

Fig. 11 represents the variation of buckling load factor k for square plate having concentric circular cutout β subjected to uniaxial loading. Here, increasing the thickness ratio and cutout ratio causes linear decrease in k . But, the value of k is more compared to that of simply supported boundary condition because, high rigidity yields to more stiffening effect along the edges during the presence of the concentric cutout. The plate having concentric circular cutout, for $\eta=0.01$

and for β ranges from 0.1 to 0.4, buckles at loads higher than the buckling load for corresponding plate without a cutout. This behavior is counterintuitive at first glance, studied for many years and experimentally verified for isotropic plates [5]. The percentage reduction of k increases with increase in η and β especially for $\beta > 0.4$ i.e., at $\beta=0.6$ and $\eta=0.3$, k decreases to 77% of its value compared to $\beta=0.1$. Fig. 12 represents the variation of buckling load factor k for square plate having concentric circular cutout β subjected to biaxial loading. Here also k is almost half of that of uniaxial compression value. There is a rapid decrease in k as η and β increases. When $\beta=0.6$, k decreases to 60% at $\eta=0.3$ when compared to $\eta=0.01$.

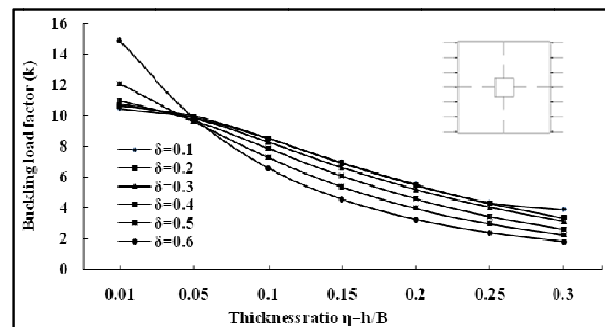


Fig. 13 Variation of k with η and δ for uniaxial compression

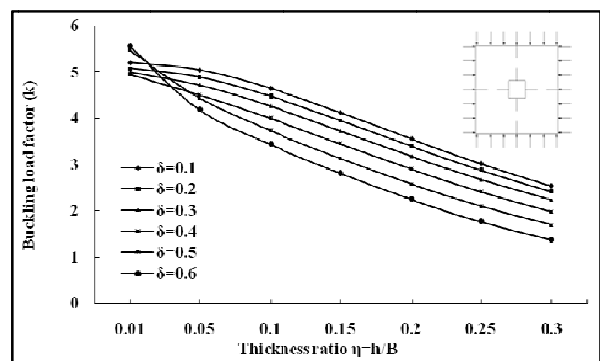


Fig. 14 Variation of k with η and δ for uniaxial compression

Fig. 13 represents the variation of buckling load factor k for square plate having concentric square cutout δ subjected to uniaxial loading. Here, also an increase of 42% in k value can be observed at $\delta = 0.6$ for $\eta=0.01$. At $\eta=0.05$, k value for all cutout ratios get coincides, this shows that increase in the cut out ratio has negligible effect on k . It is also noticed that high fluctuation of k when $\delta > 0.4$ even at $\eta=0.01$ to 0.3, similar to that of simply supported uniaxial case. Fig. 14 represents the variation of k for square plate having concentric square cutout subjected to biaxial loading. Here, k decreases with the increase of η and δ . k reduction is nearly 50% to that of the uniaxial case. k reduces up to 51%, 52%, 55%, 60%, 69% and 75% with respect to $\delta=0.1$ to 0.6 for $\eta=0.01$ to 0.3 respectively.

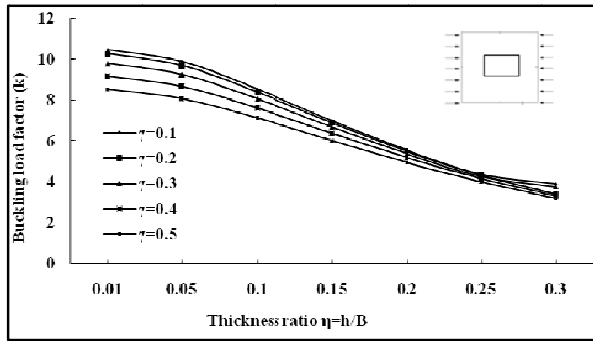
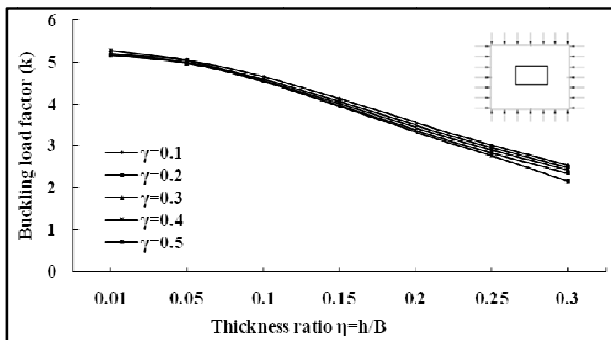
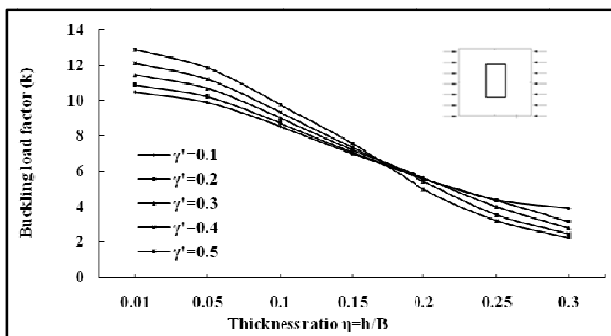
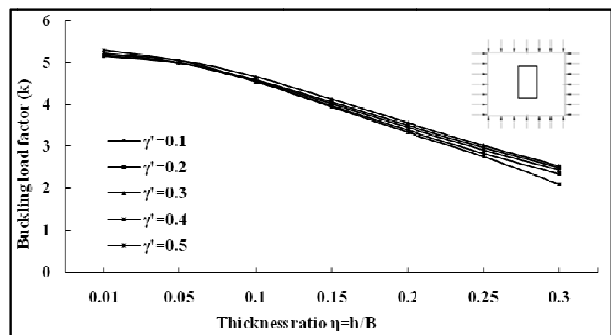
Fig. 15 Variation of k with η and γ for uniaxial compressionFig. 16 Variation of k with η and γ for biaxial compressionFig. 17 Variation of k with η and γ' for uniaxial compressionFig. 18 Variation of k with η and γ' for biaxial compression

Fig. 15 represents the variation of buckling load factor k for square plate having concentric rectangular cutout along x -

direction γ subjected to uniaxial loading. Here, it is observed that significant reduction of k up to $\eta=0.15$ for all increasing γ values and then onwards reduction in k remains the same for $\eta > 0.15$. Fig. 17 represents the variation of k for square plate having concentric rectangular cutout along y -direction γ' subjected to uniaxial loading. Here, significant reduction of k is observed as the increase of η values with the increase of γ' values and it is noticed that the k reduction is 63 to 83% when $\eta=0.01$ to 0.3 and $\gamma'=0.1$ to 0.5 . γ' values merged between $\eta=0.15$ to 0.2 . Figs. 16 and 18 represent the variation of buckling load factor k for square plate having concentric rectangular cutout along x and y directions subjected to biaxial loading. Almost k value overlaps and decreases as η , γ and γ' increases in rectangular cutout both along x and y directions.

D. Case of Plate with SCSC Boundary Conditions

Figs. 19-26 show the variation of the buckling load factor k for the plate with different cutout ratios having SCSC plate boundary conditions subjected to inplane uniaxial and biaxial compression loading cases. In all these figures the variation of the buckling load factor k are plotted against thickness ratio η and cutout ratios. It can be noticed in these figures that, buckling behavior of the plate is greatly affected by increase in plate thickness ratios. The buckling load factor k for SCSC plate lies between the simply supported and clamped plate boundary conditions but variation of buckling load factor k is very much resemblance to the clamped plate boundary condition.

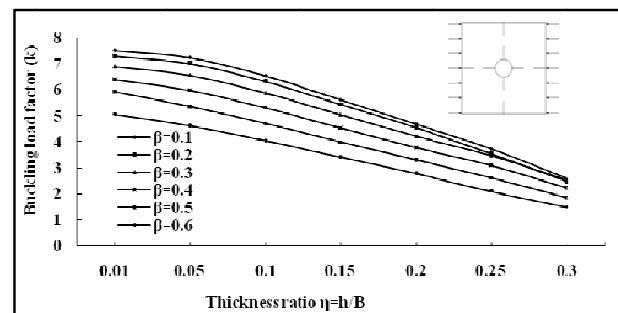
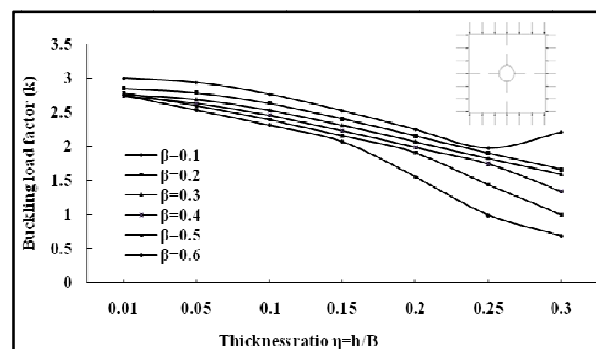
Fig. 19 Variation of k with η and β for uniaxial compressionFig. 20 Variation of k with η and β for biaxial compression

Fig. 19, the buckling load factor k decreases with increase

in cutout ratios β and thickness ratio η . Buckling load factor k decreases to 60-70% as η increases from 0.01 to 0.3. Reduction is 25% for $\beta = 0.1$ to 0.3 at $\eta = 0.15$, but for $\beta > 0.3$ it reaches to 33% in circular cutout. This clearly indicates that at larger cutouts increase of plate thickness ratio does not influence the buckling strength. In biaxial compression for circular cutout k decreases linearly as η and β increases, when $\eta > 0.15$ and $\beta > 0.4$, k decreases in rapid manner, Fig. 20.

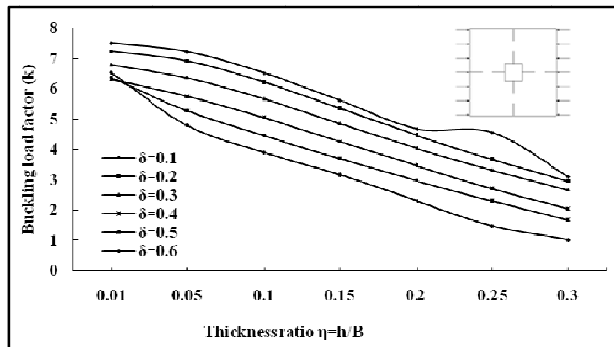


Fig. 21 Variation of k with η and δ for uniaxial compression

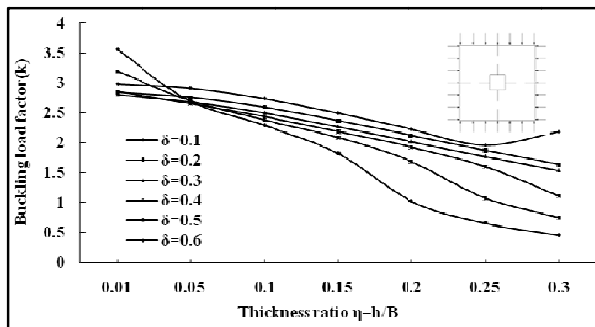


Fig. 22 Variation of k with η and δ biaxial compression

Fig. 21, here, also k decreases with increase in δ and η , the reduction is 59-85%. At $\eta = 0.15$, 25% reduction is observed for β up to 0.2 but when $\beta \geq 0.3$, reduction reaches to 52%. In Fig. 22, k decreases as η and δ increases, here variation of k is very much unpredictable when $\delta > 0.4$ in which the variation of k starts from very beginning and decreases in more rapid manner with the increase of η .

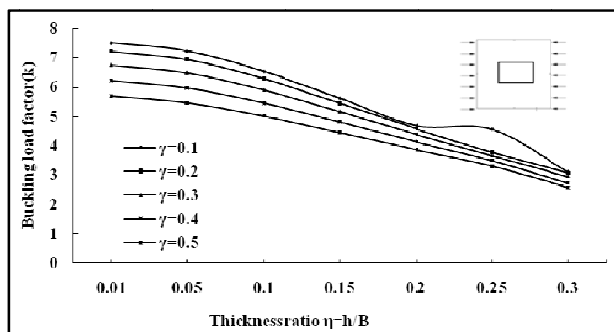


Fig. 23 Variation of k with η and γ for uniaxial compression

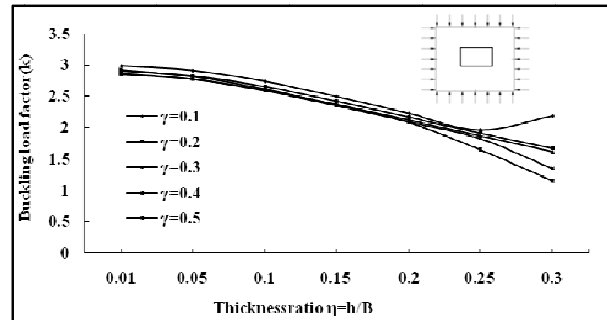


Fig. 24 Variation of k with η and γ for biaxial compression

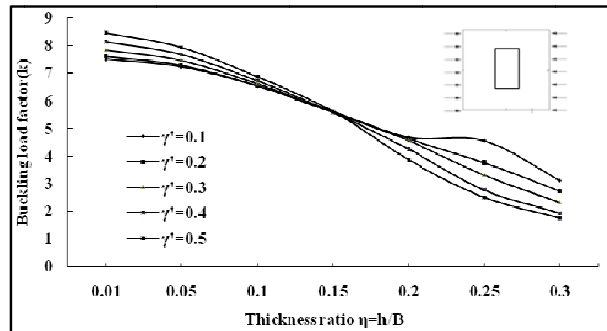


Fig. 25 Variation of k with η and γ' for uniaxial compression

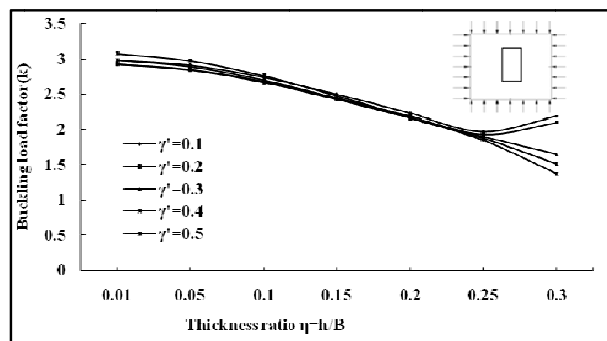


Fig. 26 Variation of k with η and γ' for biaxial compression

Fig. 23, in case of rectangular cutout along x-direction, k reduces to 25% at $\eta = 0.15$ and reaches to 55-58% for increase in η up to 0.3 for all cutout ratios. Here, the rate of reduction of k is less compared to circular and square cutouts. Fig. 25, in case of rectangular cutout along y-direction k decreases with increase in γ' , for η up to 0.15. It is also observed that for $\eta = 0.15$, k value for all cutout ratio merges. This may be the indication of the transition point where high k reduction due to increase of η for all values of γ' . In Figs. 24 and 26, k reduces with respect to η and cutout ratios γ and γ' and k value nearly overlaps up to $\eta < 0.25$ for all cutout ratios.

V. CONCLUSION

A study of buckling behavior of uniformly compressed isotropic square plate with different shape and size of the cutouts, investigated using FEM are presented in this paper.

Square plates having SSSS, CCCC and SCSC boundary conditions with wide ranges of cutout ratios and plate thickness ratios are considered. The following conclusions are drawn.

- 1) Buckling is the critical mode of failure for the major portion of the compressed plate with cutout especially when its thickness is considerably small.
- 2) The cutouts have considerable influence on the buckling load factor k . The effect is larger in higher cutout ratios and for plate thickness ratio greater than 0.15.
- 3) Square plate having circular and square cutouts exhibits similar behavior under uniaxial and biaxial loadings, but, plate with circular cutouts is more efficient compare to plate with square cutouts.
- 4) In the plate with circular cutout and square cutout, buckling load factor k gradually decreases with the increase of thickness ratio η and cutout ratios β and δ . The value of k is less by 10% in case of square cutout compared to circular cutout for SSSS plate boundary condition and it is 5-10% in CCCC and SCSC cases.
- 5) Square plate with rectangular cutout, along x -direction, shows reduction in the buckling load factor k and it is up to 18% in CCCC and more than 20% in SSSS and SCSC cases.
- 6) In case of biaxial loading, buckling load factor k value is found to be almost half of that of uniaxial compression value, since stiffening of the plate occurs in two directions.

In summary, buckling of plates with interior cutouts is very much affected with the plate thickness and boundary conditions. The current study offers useful information for the designers.

REFERENCES

- [1] ANSYS, User Manual, Version 10.0, Ansys Inc.
- [2] Aydin Komur, M., Mustafas Sonmez., "Elastic buckling of rectangular plates under linearly varying in-plane normal load ratio with a circular cutout", *Mechanics Research Communications*, vol.35, pp.361-371, 2008.
- [3] Chiang-Nan Chang, and Feung-Kung Chiang, "Stability analysis of a thick plate with interior cutout", *AIAA Journal*, vol.28, no. 7, pp.1285-1291, 1990.
- [4] Christopher J. Brown, Alan L. Yettram, and Mark Burnett, "Stability of plates with rectangular holes", *Journal of Structural Engineering*, vol.113, no 5, pp.1111-1116, 1987.
- [5] El-Sawy K.M., Nazmy A.S., "Effect of aspect ratio on the elastic buckling of uniaxially loaded plates with eccentric holes", *Thin Walled Structures*, vol.39, pp.983-998, 2001.
- [6] Herrmann, G., and Armenakas, A.E., "Vibration and stability of plates under initial stress", *Journal of Engineering Mechanics, ASCE*, vol.86, no.EM3, pp.65-94, June 1960.
- [7] Jeom Kee Paik, "Ultimate strength of perforated steel plate under combined biaxial compression and edge shear loads", *Thin-Walled Structures*, vol.46, pp.207-213, 2008..
- [8] Sabir A. B., and Chow F.Y., "Elastic buckling containing eccentrically located circular holes", *Thin-Walled Structures*, vol.4, pp.135-149, 1986.
- [9] Shakerley T.M., Brown C.J., "Elastic Buckling of Plates with Eccentrically Positioned Rectangular Perforations". *Int. Journal of Mechanical Sciences*, vol. 38(8-9), pp.825-838, 1996.
- [10] Shanmugam N.E., Thevendran V, Tan Y.H., "Design formula for axially compressed perforated plates", *Thin-Walled Structures*, vol.34(1), pp.1-20, 1999.
- [11] Srinivas S., and Rao A.K., "Buckling of thick rectangular plates", *AIAA Journal*, vol.7, pp.1645 - 1647, 1969.
- [12] Suneel Kumar M. P., Alagusundaramoorthy, Sundaravadivelu R., "Ultimate strength of square plate with rectangular opening under axial compression", *Journal of Naval Architecture and Marine Engineering*, pp.15-26, 2007.
- [13] Timoshenko S.P., and James M. Gere., "*Theory of Elastic Stability*", second ed. McGraw- Hill company, Singapore, 1963, pp.348-389.
- [14] Yettram A.L., and Brown C.J., "The elastic stability of square perforated plates under biaxial loading", *Computers and Structures*, vol.22, no.4, pp.589-594, 1986.